Biol. Cybern. 84, 425–434 (2001)

Biological Cybernetics


# Biomechanical analysis of movement strategies in human forward trunk bending. I. Modeling

**A. V. Alexandrov**[1], **A. A. Frolov**[1], **J. Massion**[2,3]

[1] Institute of Higher Nervous Activity and Neurophysiology, Russian Academy of Science, 5A Butlerov, Moscow 117865, Russia
[2] Laboratory of Neurobiology and Movements, CNRS, 31 chemin Joseph Aiguier, 13402 Marseille Cedex 20, France
[3] Laboratoire Parole et Langage, Université de Provence, 29, av. Robert Schuman, 13621 Aixen Provence, France

Received: 1 July 1999 / Accepted in revised form: 23 October 2000

**Abstract.** Two behavioral goals are achieved simultaneously during forward trunk bending in humans: the bending movement per se and equilibrium maintenance. The objective of the present study was to understand how the two goals are achieved by using a biomechanical model of this task. Since keeping the center of pressure inside the support area is a crucial condition for equilibrium maintenance during the movement, we decided to model an extreme case, called "optimal bending", in which the movement is performed without any center of pressure displacement at all, as if standing on an extremely narrow support. The "optimal bending" is used as a reference in the analysis of experimental data in a companion paper. The study is based on a three-joint (ankle, knee, and hip) model of the human body and is performed in terms of "eigenmovements", i.e., the movements along eigenvectors of the motion equation. They are termed "ankle", "hip", and "knee" eigenmovements according to the dominant joint that provides the largest contribution to the corresponding eigenmovement. The advantage of the eigenmovement approach is the presentation of the coupled system of dynamic equations in the form of three independent motion equations. Each of these equations is equivalent to the motion equation for an inverted pendulum. Optimal bending is constructed as a superposition of two (hip and ankle) eigenmovements. The hip eigenmovement contributes the most to the movement kinematics, whereas the contributions of both eigenmovements into the movement dynamics are comparable. The ankle eigenmovement moves the center of gravity forward and compensates for the backward center of gravity shift that is provoked by trunk bending as a result of dynamic interactions between body segments. An important characteristic of the optimal bending is the timing of the onset of each eigenmovement: the ankle eigenmovement onset precedes that of the hip eigenmovement. Without an earlier onset of the ankle eigenmovement, forward bending on the extremely narrow support results in falling backward. This modeling approach suggests that during trunk bending, two motion units – the hip and ankle eigenmovements – are responsible for the movement and for equilibrium maintenance, respectively.

*Correspondence to*: A. V. Alexandrov
(Tel.: +7-95-334-7749, Fax: +7-95-338-8500,
e-mail: labdo@mail.ru)

## 1 Introduction

Maintenance of dynamic equilibrium requires efficient control strategies to master the many degrees of freedom in order to achieve the whole body stabilization. This is particularly evident for humans performing movements while standing. Raising an arm or bending the trunk cause dynamic interactions between segments which, in absence of adequate compensations, would result in falling (Ramos and Stark 1990) or in marked changes in the body geometry (Eng et al. 1992). How the control exerted by the central nervous system (CNS) is organized in order to perform the movement and maintain equilibrium is still a matter of discussion. There are two main theories for explaining how the central control for coordinating these two tasks is organized. One of the theories suggests that the CNS controls the movement and equilibrium maintenance as a single process. This could be performed according to two main hypotheses. A first one is represented by the equilibrium point model and the second one by the inverse dynamic model. In the equilibrium point model (Bizzi et al. 1992; Latash 1993; Feldman and Levin 1995), the CNS controls only equilibrium body states. Transition from initial to final posture (i.e., the movement) is provoked by a single central signal which defines a new final body configuration (Feldman and Levin 1995). This model suggests that dynamic interaction between segments is automatically compensated due to the viscoelastic properties of the neuromuscular apparatus and that the CNS does not have to take into account these interactions in the

movement control. In contrast with this view, in the inverse dynamic model the expected coupling torques are calculated explicitly and activation patterns for individual muscles are generated to compensate in advance for the expected perturbations (Kawato et al. 1987). In this case, the central command predicts all forthcoming posture perturbations and therefore does not need posture corrections. In spite of the differences in the central command generation, both these models treat the movement and equilibrium maintenance as a single process. A second theory proposes two parallel independent controls of the two movement components: prime (focal) and associated (postural) movements (for review see Massion 1992). The prime movement serves the main behavioral goal whereas the associated movement counteracts dynamic posture perturbations produced by the prime movement. Usually, the associated movement precedes the voluntary prime movement. This implies that the associated movement is pre-programmed and could be considered as an integral part of a central motor program (Bouisset and Zattara 1987).

Fast human trunk bending in the sagittal plane seems to be a good behavioral model to reveal the rules of coordination between movement and posture, because in this movement such coordination is especially important. The fast displacement of the heavy trunk produces a large equilibrium disturbance while the support is limited by the relatively small feet size. During the performance of the task, the center of pressure (CP) as well as the center of gravity (CG) are kept within safety margins along the anteroposterior axis. Axial synergies, i.e., opposite displacements of the upper and lower body segments, have been thought as responsible for the minimization of the CG shift (Babinski 1899). In a previous paper, using a prinicipal component kinematic analysis of these axial synergies (Alexandrov et al. 1998), it was proposed that a single central control is applied to the various joints of the kinematic chain, ensuring both the trunk movement and the equilibrium maintenance. This work was in favor of the equilibrium point hypothesis as proposed by Feldman and Levin (1995). However, the conclusion was reached by using an analysis restricted to the kinematics. It did not explain how the complex dynamic interactions between segments were compensated during trunk bending and how the CNS was actively involved in this compensation. In particular, the pure kinematic analysis did not explain the electromyographic (EMG) pattern observed in forward upper trunk bending. The bending is usually preceded by an activation of tibialis anterior and/or an inhibition of the soleus (Oddsson and Thorstensson 1986, 1987, 1990; Crenna et al. 1987, 1988; Pedotti et al. 1989). The EMG pattern at the ankle joint has been interpreted as being related to an associated movement aimed to compensate in advance for equilibrium disturbance provoked by the forthcoming hip flexion, considered a prime movement (Oddsson and Thorstensson 1986). However, this early ankle muscle activity cannot be considered as compensatory for the forthcoming posture perturbation due to hip flexion per se, because such activity provokes CG displacement in the same (forward) direction as hip flexion. A more thorough analysis is therefore required to understand how prime and associated movements are coordinated in the trunk forward bending.

In the present study we propose a biomechanical analysis of kinematic as well as dynamic aspects of trunk bending movement in order to better understand the mechanisms of coordination between movement and posture in this task. In a first step, which is developed in the present paper, we propose an analysis based on computer simulations. Since keeping the CP and the projection of the CG inside the support area is essential for equilibrium, we model a trunk bending movement where one or the other of these two reference values are kept constant during the whole movement. Thus, from a biomechanical point of view, two "ideal" trunk bending movements were modeled, a movement with complete stabilization either of the CG (Bouisset and Zattara 1987; Massion 1992; Massion et al. 1997; Domen et al. 1999) or a movement with complete stabilization of the CP (Do and Gilles 1992). The main goal of the present study is to describe the biomechanical peculiarities of both these "ideal" movements.

The analysis is based on a three-joint (ankle, knee, and hip) biomechanical model of the human body (Barin 1989; Yang et al. 1990; Kuo and Zajac 1993). It is carried out in the linear approximation which allows decomposition of the movement into three "eigenmovements" along the eigenvectors of the motion equation. Each eigenmovement is a multijoint movement involving the hip, knee, and ankle joints. By definition, in eigenmovement (in contrast to any other movement) the linear relationship between the joint angles is accompanied by a linear relationship between joint torques. Each eigenmovement appears to have a dominant joint (ankle, hip, or knee) which contributes the most to eigenmovement kinematics and dynamics, and therefore they are termed in this study "ankle" (A), "hip" (H), and "knee" (K) eigenmovements. It is shown that in both "ideal" movements, H-eigenmovement alone almost completely describes the whole movement kinematics. For the movement dynamics, two eigenmovements (A and H) are important. The eigenmovement approach allows to split the coupled system of dynamic equations into independent equations and therefore to construct the desired "ideal" movements in the easiest way. Particularly, it avoids tedious calculations of joint torques which ensure forward trunk bending without any CG or CP displacements.

It will be shown that reducing the CG displacement to zero requires large CP displacements which are not compatible with experimental data. Therefore, the most detailed analyses relate to the second ideal movement, i.e., bending without CP displacement. This bending is termed below as "optimal" one because in principle it can be performed without equilibrium loss while standing on an extremely narrow support. Neither biomechanical peculiarities of such bending nor even its theoretical possibility are obvious. As it will be shown, this movement is possible but it requires very precise coordination between internal muscle forces and exter-

nal gravitational forces. In particular, the movement has to start with a forward CG acceleration in A-eigenmovement which compensates in advance for the forthcoming backward CG displacement in H-eigenmovement.

This coordination between H- and A-eigenmovements leads us to the suggestion that these eigenmovements are the prime and the postural movement components, respectively. First, as a prime movement, the H-eigenmovement almost completely describes the movement kinematics. Second, this eigenmovement is accompanied by a backward CG displacement which requires a compensation by the postural movement component (A-eigenmovement) producing a forward CG shift. The results of the biomechanical modeling are in line with the observed EMG pattern mentioned above.

In Alexandrov et al. (2001) this suggestion is considered further. In particular, it is shown that the peculiarities of the hypothetical bending on the extremely narrow support described here are illustrative of the experimental bending performed on a support of small but finite size.

## 2 Biomechanical model of forward trunk bending

In the present study, human dynamics in the sagittal plane are represented as an open-chain three-link inverted pendulum (Barin 1989; Yang et al. 1990; Kuo and Zajac 1993), placed on a triangular foot (Gurfinkel 1973). As shown in Fig. 1, the foot is assumed to be motionless with respect to the support. Body segments are assumed to be thin rigid links rotating about three ideal pin joints – hip, ankle, and knee – with a torque actuator at each joint.

The motion equation of a three-rigid-link system under the gravity force is:

$$\mathbf{C}(\varphi)\ddot{\varphi} - \mathbf{D}(\varphi)\varphi + \mathbf{A}(\varphi, \dot{\varphi}) = \mathbf{T} \tag{1}$$

where $\varphi$ is the vector of hip, knee, and ankle joint angles, and $\mathbf{T}$ is the vector of joint torques. In vectors $\varphi$ and $\mathbf{T}$ the first component relates to the ankle, the second to the knee, and the third to the hip. $\mathbf{C}$ and $\mathbf{D}$ are inertia and gravitational matrices, and vector $\mathbf{A}$ defines centripetal and Coriolis forces.

To specify the elements of matrices $\mathbf{C}$ and $\mathbf{D}$ and the components of vector $\mathbf{A}$ (Appendix A), one needs to know four anthropometric parameters of each of the three body segments: the length, mass, and location of the centers of mass with respect to the distal end, and the moment of inertia with respect to the center of mass.

The most complete and transparent analysis of the motion equation (1) can be carried out in the linear approximation (Barin 1989). Equation (1) can be linearized with high precision up to the trunk bending of 60° (Appendix B). In the linear approximation it takes the form

$$\mathbf{C}\ddot{\varphi} - \mathbf{D}\varphi = \mathbf{T} \tag{2}$$

where, in contrast to (1), inertia matrix $\mathbf{C}$ and gravitational matrix $\mathbf{D}$ are angle independent (Appendix A). The linear approach allows decomposition of any three-joint movement into three components (“eigenmovements”), each one representing a movement along one of the three eigenvectors $\mathbf{w}_i$ of the linear motion equation (2), which are defined by

$$\mathbf{C}\mathbf{w}_i = \lambda_i \mathbf{D}\mathbf{w}_i \tag{3}$$

where $\lambda_i$ are corresponding eigenvalues. Subscripts $i$ = A,H,K correspond to the dominant component (of ankle, hip, or knee joints) in each eigenvector; see (10).

The presentation of the movement in terms of eigenmovements implies the transformation of the vector of joint angles $\varphi(t)$ into the vector of eigenmovement “kinematic scaling amplitudes” $\xi(t)$:

$$\varphi(t) = \mathbf{W}\xi(t) \tag{4}$$

where columns of matrix $\mathbf{W}$ are eigenvectors $\mathbf{w}_i$ and each component of vector $\xi(t)$ defines the time course of the movement along each eigenvector (eigenmovement).

The “dynamic scaling amplitude” $\eta_i$ of each eigenmovement is calculated by inserting (4) into (2). Taking

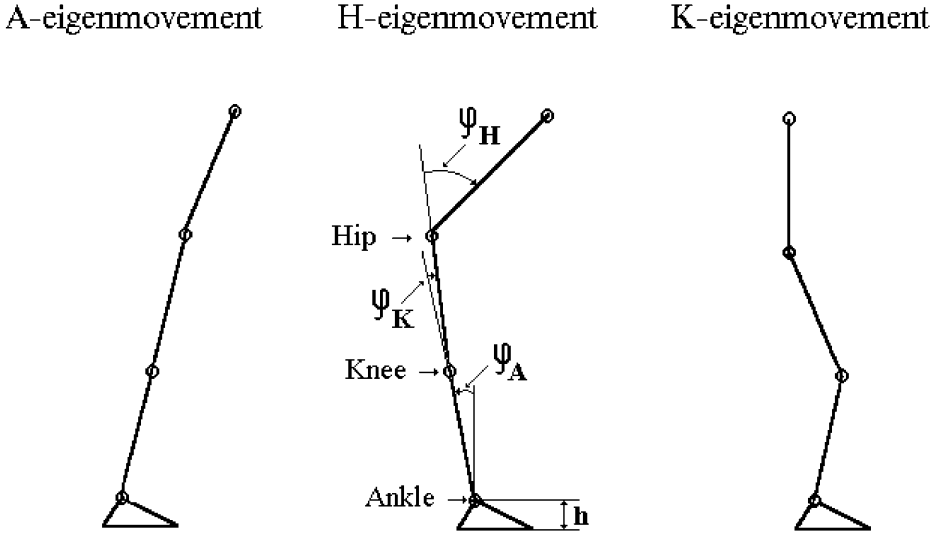


**Fig. 1.** Three-link model of the human body. Joint angles in the ankle, knee, and hip are represented by $\varphi_A, \varphi_K$, and $\varphi_H$. Three stick diagrams represent kinematic patterns described by ankle (A), hip(H), and knee (K) eigenvectors shown in (10)

into account (3), one obtains three independent dynamic equations for each eigenmovement:

$$-\lambda_i \ddot{\xi}_i + \xi_i = \eta_i \tag{5}$$

and the vector of joint torques **T** is defined by the vector of dynamic scaling amplitudes $\eta$ according to

$$\mathbf{T}(t) = \mathbf{U}\eta(t) \tag{6}$$

where matrix $\mathbf{U} = -\mathbf{DW}$ defines the contribution of each eigenmovement to the total joint torques.

The advantage of the analysis of the motion equation in terms of eigenmovements is the splitting of the coupled dynamic equation (2) into three simple independent motion equations (5). Each of these equations is equivalent to the motion equation for an inverted pendulum with inertia $\lambda_i$. As a consequence (Appendix C), it is possible to calculate the resulting CP and CG positions – $X_i^{CG}$ and $X_i^{CP}$ – in each eigenmovement in which their relationship takes a simple form:

$$-(\lambda_i + h/g)\ddot{X}_i^{CG} + X_i^{CG} = X_i^{CP} \tag{7}$$

where $h$ is the distance between the ankle joint and the support (feet height, Fig. 1) and $g$ is the gravity acceleration. In the simulations, the distance $h$ for a "standard human" was taken to be 5 cm.

Equation (7) is the basis for the analysis of the trunk bending carried out in the present study. The respective changes in CP and CG positions, which are of special importance for equilibrium maintenance, will be analyzed. The relationship between $X_i^{CG}$ and the corresponding kinematic scaling amplitude $\xi_i$ is

$$X_i^{CG} = b_i \xi_i \tag{8}$$

where coefficients $b_i$ are defined by human anthropometric parameters (Appendix C).

For a "standard human" of 70-kg body mass and 170-cm height, with standardized anthropometric parameters of the body segments (Winter 1990), the solution of (3) gives the following eigenvalues for A-, H- and K-eigenmovements:

$$\lambda_A = 0.108\,s^2,\ \ \lambda_H = 0.020\,s^2,\ \ \lambda_K = 0.0021\,s^2 \tag{9}$$

the following eigenvectors (columns of matrix **W** in Eq. 4):

$$\mathbf{w}_A = \begin{pmatrix} -0.94 \\ -0.09 \\ -0.32 \end{pmatrix},\ \ \mathbf{w}_H = \begin{pmatrix} -0.24 \\ 0.06 \\ 0.97 \end{pmatrix},\ \ \mathbf{w}_K = \begin{pmatrix} -0.33 \\ 0.80 \\ -0.52 \end{pmatrix} \tag{10}$$

and the following columns of matrix **U** in (6):

$$\mathbf{u}_A = \begin{pmatrix} 668.4 \\ 382.5 \\ 143.1 \end{pmatrix},\ \ \mathbf{u}_H = \begin{pmatrix} 32.1 \\ -41.4 \\ -83.4 \end{pmatrix},\ \ \mathbf{u}_K = \begin{pmatrix} 6.3 \\ -96.0 \\ 7.7 \end{pmatrix} \tag{11}$$

Vectors $\mathbf{w}_i$ and $\mathbf{u}_i (i = A,H,K)$ in (10) and (11) are ordered by the increasing eigenvalue $\lambda_i$ (eigenmovement inertia). The components of these vectors (the relative weights of each joint in a given eigenmovement) correspond to the ankle, knee, and hip joints from top to bottom. The three eigenmovements are termed A-, H- and K-eigenmovements according to the joint which has the largest component in eigenvectors $\mathbf{w}_i$ and in vectors $\mathbf{u}_i$, and thus contributes the most to the eigenmovement kinematics ($\mathbf{w}_i$) as well as dynamics ($\mathbf{u}_i$).

The coefficients $b_i (i = A,K,H)$ in (8) defining the displacement of the CG as a function of the kinematic scaling amplitude $\xi_i$ in each eigenmovement are the following:

$$b_A = 1.636\ \text{cm/deg}, \quad b_H = 0.079\ \text{cm/deg}, \quad b_K = 0.015\ \text{cm/deg} \tag{12}$$

The kinematic pattern of A-eigenmovement (given by eigenvector $\mathbf{w}_A$) is close to the whole body rotation around the ankle joint (Fig. 1, left). The kinematic pattern of H-eigenmovement ($\mathbf{w}_H$) is close to the forward trunk bending which is accompanied by opposite displacements of upper and lower segments (Fig. 1, middle). The kinematic pattern of K-eigenmovement ($\mathbf{w}_K$) is close to a sitting down movement with knee flexion and an almost vertical translational movement of the trunk segment (Fig. 1, right).

Figure 2 illustrates the relationships between CG and CP displacements and the corresponding scaling amplitudes $\xi_i$ in the eigenmovements with a "typical" bell-shaped CG velocity profile

$$\dot{X}^{CG}(t) = VF[(2(t - t_0)/\tau - 1)^2] \tag{13}$$

where $V$, $t_0$, and $\tau$ are the peak velocity, the onset, and the duration of CG displacement in the eigenmovement, respectively, and $F(\gamma)$ is a bell-shaped function given by a polynomial of fourth order so that

$$F(\gamma) = 1 + \sum_{i=1}^{4} a_i \gamma^i \quad \text{for } |\gamma| < 1,$$

$$F(\gamma) = 0 \quad \text{for } |\gamma| > 1\ .$$

Coefficients $a_i$ are chosen as $a_1 = -2.6, a_2 = 5.2, a_3 = -3.6, a_4 = 1$ to fit the velocity time profile during experimental trunk bending. Under the given parameters, the CG shift amounts to $\Delta X^{CG} = 0.51\,V\tau$, which corresponds to the values of experimental bending (see Alexandrov et al. 2001).

In each eigenmovement shown in Fig. 2, the CG shift amplitude onset and duration were taken $\Delta X^{CG} = 1$ cm, $t_0 = 0$ and $\tau = 500$ ms. The initial CP shift is first directed backward and exerts a forward CG acceleration, thus in a direction opposite to CP shift (Fig. 2A). Thereafter the CP moves forward and goes beyond the CG, which is decelerated. Since the inertia of the A-eigenmovement is the highest, the CP excursion in this eigenmovement is the largest (6.5 cm). By contrast, in K-eigenmovement with the lowest inertia, the CP

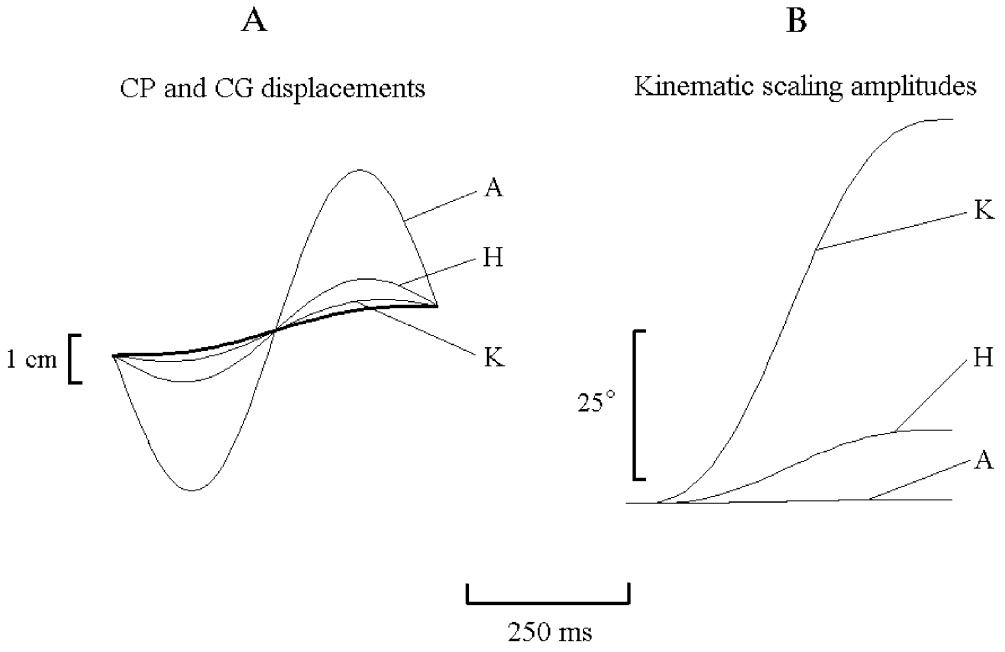


**Fig. 2A,B.** Center of pressure (CP) displacement and eigenmovement amplitude which produce a forward center of gravity (CG) displacement of 1 cm for 500 ms movement are represented for A-, H- and K-eigenmovements: **A** *thick line*: CG displacement, *thin lines*: CP displacements in corresponding eigenmovements; **B** kinematic scaling amplitudes (time courses $\xi_i(t)$, see text) of the corresponding eigenmovements

excursion is the smallest (1.2 cm), and the CP time course is similar to that of the CG. At the first sight K-eigenmovement seems to be the most efficient in equilibrium regulation, because a smaller size of support is required to produce a given CG displacement. However, according to (12), the CG displacement in K-eigenmovement is accompanied by the largest movement amplitude. For example a CG shift of 1 cm corresponds (Fig. 2B) to a movement of 65° in K-eigenmovement (52° of knee flexion) and only to 0.61° in A-eigenmovement (0.58° of ankle flexion). Thus, A-eigenmovement is the most efficient at producing *slow and large* CG shifts, and K-eigenmovement is the most efficient to produce *fast and small* CG shifts.

In the experimental forward bending, the amplitude of K-eigenmovement is small and the mean CG displacement in K-eigenmovement amounted only to 0.1 cm, whereas in A- and H- eigenmovements it amounted to 4.9 cm and 4.5 cm, respectively (see Alexandrov et al. 2001). Thus the contribution of K-eigenmovement to equilibrium maintenance during human forward bending appeared to be negligible. Taking this into account, we ignore the K-eigenmovement in the modeling described in the following section.

## 3 "Ideal" trunk bending movements

In Sect. 2 we identified during forward trunk bending three linear biomechanical synergies (eigenmovements), each one involving ankle, knee, and hip joints, and we illustrated their potential contributions to the control of CG. Since the contribution of the K-eigenmovement is negligible, the aim of this part of the modeling is to see how the coordination between the H- and A-eigenmovements provides for different patterns of CP and CG displacements. For this purpose, we simulate two extreme conditions: (1) trunk bending without CG displacement, and (2) trunk bending without CP displacement. The idea of the modeling procedure is as follows. First we take a bending movement described by an H-eigenvector (Fig. 1, middle) with a "typical" velocity profile (13). Then we "add" an A-eigenmovement with proper parameters (Fig. 1, left) to this movement in order to compensate for either CG or CP displacements induced by the chosen H-eigenmovement. In both "ideal" movements, the CG shift in A-eigenmovement is equal by absolute value to that in H-eigenmovement. Since coefficient $b_A$ is about 20 times larger than $b_H$ (see Eq. 12), then according to (8) the amplitudes of A-eigenmovement in both "ideal" movements are about 20 times smaller than those of H-eigenmovement. This means that more than 95% of the angular variance in these movements is explained by H-eigenmovement.

Let the CG displacement in H-eigenmovement have a "typical" bell-shaped velocity profile given by (13) where, according to experimental data (see Alexandrov et al. 2001), $\tau_H = 510$ ms, $t_{0H} = 390$ ms, and $\Delta X_H^{CG} = 4.5$ cm. The "typical" CG movement in forward trunk bending performed along H-eigenvector $\mathbf{w}_H$ is shown in Fig. 3A (left, thick line) as calculated by (13).

### *3.1 Bending without CG displacement*

Let us first consider the bending without any CG displacement. The initial zero positions $X_i^{CG}(0) = 0$, $X_i^{CP}(0) = 0 (i = A,H)$ of the CG and the CP for both eigenmovements are assumed to correspond to initial vertical standing with the ankle joint at zero position. To compensate for the CG displacement in H-eigenmovement, the A-eigenmovement must provide the opposite CG displacement: $X_A^{CG} = -X_H^{CG}$. Displacements of the CP in H- and A-eigenmovements are calculated by using (7). They are shown in Fig. 3A along with correspond-

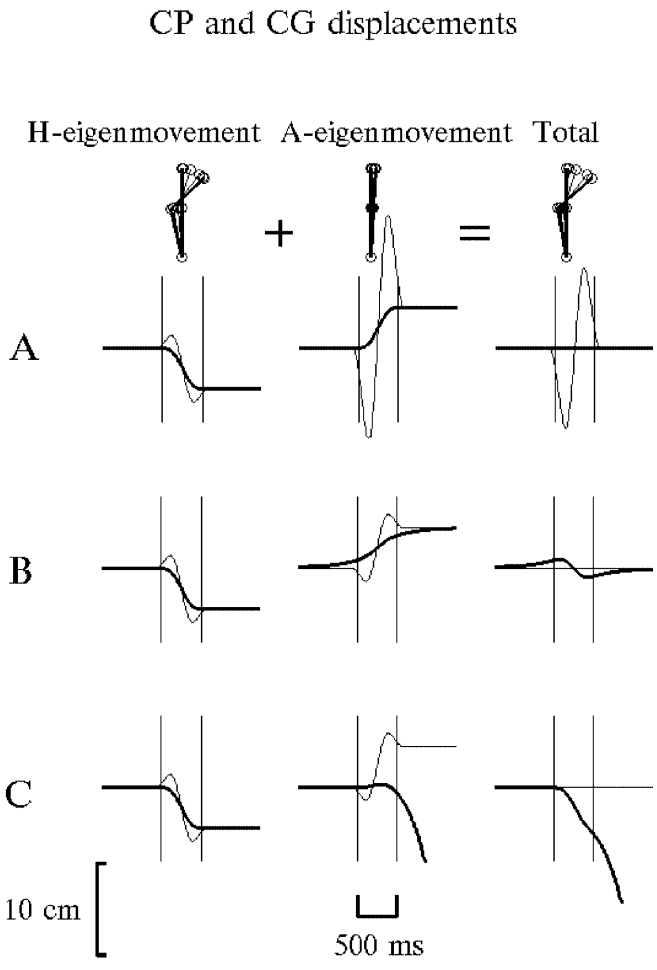


**Fig. 3A–C.** Displacements of CP (*thin lines*) and CG (*thick lines*) in three types of simulated bendings. Total displacements (*right*) are decomposed into corresponding displacements in H-eigenmovements (*left*) and A-eigenmovements (*middle*). The stick diagrams illustrate eigenmovement kinematic patterns. The knee joint and K-eigenmovement are not shown due to their weak contribution into human forward bending: **A** movement without CG displacement, **B, C** movement without CP displacement (**B** with and **C** without anticipatory forward CG displacement in A-eigenmovement). Note that in **C** the subject falls backward. *Vertical bars* in all graphics indicate onsets and offsets of H-eigenmovement. The H-eigenmovement was taken to be the same for all three (**A**, **B**, and **C**) types of bendings

ing CG displacements. Since the inertia of A-eigenmovement is much higher than that of H-eigenmovement, CP excursion in A-eigenmovement is much larger. Consequently, the total CP excursion amounts to 17.6 cm. This value is more than double the experimentally observed values (7.8 cm average, see Alexandrov et al. 2001). Thus, trunk bending in which the CG displacement is completely eliminated does not correspond to the actual performance as revealed by the analysis of the experimental data.

### *3.2 Bending without CP displacement (optimal bending)*

Such movement could be performed, in principle, while standing on an extremely narrow support. Let the CG displacement in H-eigenmovement again be described by (13) with the previous values of $\tau_H$, $t_{0H}$, $\Delta X_H^{CG}$ and with the same initial zero position $X_H^{CG}(0) = 0$. Fig. 3B (left) shows the same CG (thick line) and CP (thin line) displacements in H-eigenmovement, as in Fig. 3A (left). To compensate for the CP displacement in H-eigenmovement, the A-eigenmovement must have the same but opposite CP time course $X_A^{CP} = -X_H^{CP}$ (Fig. 3B, middle, thin line). Then, $X_A^{CG}$ can be found by solving (7) under boundary conditions $X_A^{CG}(-\infty) = X_A^{CG}(+\infty) = 0$, which again correspond to vertical standing in the initial and final positions. Figure 3B (middle, thick line) shows the calculated CG displacement in A-eigenmovement (middle). Figure 3B (right, thick line) shows the total CG displacement. The total CG excursion amounts to 2.0 cm in spite of the absence of CP displacement (Fig. 3B, right, thin line).

Figure 3B (middle) shows that during bending without CP displacement, the A-eigenmovement starts earlier and stops later than the H-eigenmovement (vertical bars indicate the onset and offset of H-eigenmovement). The bending consists of three phases. During the initial (before the left bar) and final (after the right bar) phases, only the A-eigenmovement is present, whereas during the middle phase both eigenmovements are superimposed. In the initial phase, the subject is "passively" falling forward under the gravity forces like an inverted pendulum. The movement initiation along eigenvector $\mathbf{w}_A$ implies the existence of three infinitesimal initial joint torques with intertorque ratios defined by vector $\mathbf{u}_A$ in (12). These torques do not affect to movement kinematics except to define the beginning of the movement. In the initial phase, the CG is located in front of the CP (the latter being always at the initial zero position) and slowly increases its velocity due to the forward directed support reaction force. During the middle phase (Fig. 3B, between bars), the initial forward CG displacement in A-eigenmovement is transiently reversed due to a backward CG displacement in H-eigenmovement (Fig. 3B, left, thick line). Consequently, the total CG is now located behind the extremely narrow support (Fig. 3B, right, thick line between bars) but continues moving forward due to the persisting A-eigenmovement velocity. In the final phase, this residual forward velocity is reduced to zero by the support reaction force braking the CG (which in this phase is located behind the CP). In this phase A-eigenmovement is similar to the movement of an inverted pendulum returning to the initial unstable equilibrium position.

It is noteworthy that in order to produce bending without CP displacement, a very precise coordination between A- and H-eigenmovements is required. This coordination is achieved by a finely tuned balance between internal muscle forces and external gravitational forces. The aim is to provide an appropriate time course of the horizontal component of the support reaction force. A precise time for the onset of the prime H-eigenmovement (left bars in Fig. 3B) must be chosen to ensure that CG forward acceleration is already sufficient to compensate for the forthcoming backward movement along the H-eigenvector. Similarly, the offset

of the H-eigenmovement (right bars in Fig. 3B) must stop exactly at the time when the CG is already posterior to the extremely narrow support, and the amount of residual forward CG velocity is just enough to return the CG to the zero position. Evidently, such finely tuned coordination between A- and H-eigenmovements is not expected in real human bending performed on a finite, though relatively small support. On the finite support however, the subject has an additional possibility for the control of CG movement: to use ankle joint torque for the CP displacements within the limits of the support.

Note that the results obtained for the total CG displacement in the "optimal" bending are valid only for the "typical" time profile of bending given by (13). Evidently, some changes in the time profile of the bending movement would result in some changes of the total CG displacement. But qualitatively the results would not change. For example, for the bending with the same amplitude and duration as in the "typical" case, but with a triangle velocity profile, the calculated total CG trajectory is indistinguishable from the trace shown in Fig. 3B.

To be sure that the obtained results were not the consequence of linearization of the motion equation, joint angles were subsequently calculated by direct solving the *nonlinear* motion equation (1). The joint torques were the same as those used in the linear case. The maximal difference between nonlinear and linear solutions amounted to 0.45° (5% of the excursion) for the ankle, 0.4° (7%) for the knee, and 3.7° (8%) for the hip joint angles. The difference between "linear" and "nonlinear" CG positions did not exceed 0.07 cm and the general pattern of movement was the same.

The following simulation proves that successful forward bending without CP displacement is possible only under the condition that forward CG acceleration *precedes* bending per se. Let H-eigenmovement (Fig. 3C, left) be the same as in Fig. 3A and B (left), and let us suppose that forward CG displacement $X_A^{CG}$ in A-eigenmovement starts from its equilibrium zero value at the same time $t_H$ as in H-eigenmovement. To provide the absence of the total CP displacement, CG displacement in A-eigenmovement must again satisfy (7), but now with the initial conditions $X_A^{CG}(t_H) = 0$ and $\dot{X}_A^{CG}(t_H) = 0$. The solution of (7) under these conditions is presented in Fig. 3C (middle). The early backward CP displacement (thin line) in A-eigenmovement provides a small forward CG displacement in this eigenmovement (thick line). But the latter – due to large inertia of A-eigenmovement – is too small to compensate for the backward CG displacement in H-eigenmovement (Fig. 3C, left, thick line). The undercompensation results in backward falling (Fig. 3C, right, thick line). Thus, forward CG acceleration due to A-eigenmovement, when occuring at the onset of H-eigenmovement, does not prevent backward falling during forward trunk bending on the extremely narrow support. The forward bending while standing on an extremely narrow support therefore can only be successful if forward CG acceleration provided by A-eigenmovement precedes the onset of H-eigenmovement as in Fig. 3B (middle).

This result is consistent with the simulation results of Ramos and Stark (1990), in spite of the fact that their study was carried out in the frame of a two-joint (hip and ankle) nonlinear model. The reasons are the following. First, the general character of the movement (falling from the beam) in our linear simulation is determined at the initial stage of the movement when nonlinear effects are evidently negligible. Second, in our simulation the movement in the knee joint is small and thus cannot drastically affect the kinematic pattern.

## 4 Discussion

Two behavioral goals are achieved simultaneously during upper trunk bending: the bending per se and equilibrium maintenance. The question raised in this paper is how these two goals are reached. In order to have an insight into the movement organization, we used a biomechanical modeling of the performance. The equilibrium can be maintained only if the CP is kept inside the relatively small support area defined by the size of the foot. To clarify the movement strategy from a biomechanical point of view, we simulated a hypothetical "optimal" bending in which the equilibrium constraint is maximal. We analyzed how the bending could be performed on an extremely narrow support, if CP does not move.

The human body is represented as three rigid links rotating around three joints (ankle, knee, and hip) in the sagittal plane. In a linear approximation, which was shown to be valid for the bending up to 50–60°, the movement is decomposed into three eigenmovements which correspond to three eigenvectors of the motion equation. Each eigenmovement includes a contribution of ankle, knee and hip joints. The main advantage of the eigenmovement approach is the splitting of a coupled system of dynamic equations into independent equations for separate eigenmovements. Each equation is similar to the motion equation for an inverted pendulum. The additional advantage of this approach is the possibility to exclude the K-eigenmovement from the biomechanical analysis because its effect on equilibrium maintenance during forward bending is negligible. The three-dimensional system can therefore be reduced to a two-dimensional system (ankle and hip eigenmovements). The analysis in terms of eigenmovements appeared to be demonstrative because the two remaining eigenmovements substantially differ in their inertias: the inertia of A-eigenmovement is five times greater than that of H-eigenmovement. Therefore, the CP excursions required to produce a given CG displacement in these eigenmovements are clearly different (Fig. 2) and the contribution of each eigenmovement to the total CP displacement can be easily separated.

The optimal bending is constructed as a reference for analysis of experimentally observed bending (see Alexandrov et al. 2001). The zero CP displacement in the optimal bending is considered as a limit case of the small displacement observed in the actual bending (Oddsson

and Thorstensson 1986; Crenna et al. 1987; Alexandrov et al. 1998). As shown, on an infinitively small support, the initial anticipatory acceleration of CG in the hypothetical optimal bending is achieved by passive falling under the gravity force. The fall is similar to the movement of an inverted pendulum moving away from the unstable equilibrium. The initial loss of equilibrium is compensated thereafter by the low-inertia H-eigenmovement which is responsible for the trunk bending, and provokes a backward CG displacement (Fig. 3). The initial forward bending cannot be provoked by an active contraction of the ankle muscles, because – due to infinitively small size of support – it would not produce any torque at the ankle joint. Therefore the passively initiated "optimal bending" should be considered a purely hypothetical case. One can expect that during voluntary trunk bending on a small (but not zero) support, the required initial CG acceleration is produced not only passively by the gravity force but also by the muscle activation at the ankle joint. This prediction is verified in Alexandrov et al. (2001).

To conclude, the biomechanical modeling of trunk bending suggests that trunk movement and equilibrium maintenance are performed by two distinct motion units or eigenmovements. The hip eigenmovement accounting for more than 95% of the movement kinematics is responsible for the trunk bending, and the ankle eigenmovement compensates for the equilibrium disturbance due to the hip eigenmovement. This point of view is further analyzed in Alexandrov et al. (2001).

*Acknowledgments.* The work was supported by Russian Foundation of Basic Research, projects 99-04-48-885 by INTAS (project INTAS-RFBR 95-1327), and by Russian Foundation of Humanity (project 00-06-00242a). The authors wish to thank Fay Horak, Marat Ioffe and Milan Zedka for their critical reading of the manuscript.

## Appendix A: Motion equation

The motion equation has a simple form in terms of segment angles $\theta_i$ with respect to the vertical:

$$\mathbf{C}'(\theta)\ddot{\theta} - \mathbf{D}'(\theta)\theta + \mathbf{A}'(\theta,\dot{\theta}) = \mathbf{NT} \qquad \text{(A1)}$$

where $\mathbf{T}$ is the vector of joint torques. Matrix $\mathbf{N}$ is

$$\mathbf{N} = \begin{pmatrix} 1 & -1 & 0 \\ 0 & 1 & -1 \\ 0 & 0 & 1 \end{pmatrix}$$

and the elements of the inertia matrix $\mathbf{C}'(\theta)$, gravitational matrix $\mathbf{D}'(\theta)$ and components of the vector of centripetal and Coriolis forces $\mathbf{A}'(\theta,\dot{\theta})$ are

$$C'_{\mathrm{UU}} = m_{\mathrm{U}}c_{\mathrm{U}}^2 + I_{\mathrm{U}}$$

$$C'_{\mathrm{UM}} = C'_{\mathrm{MU}} = m_{\mathrm{U}}c_{\mathrm{U}}l_{\mathrm{M}}\cos(\theta_{\mathrm{U}} - \theta_{\mathrm{M}})$$

$$C'_{\mathrm{UL}} = C'_{\mathrm{LU}} = m_{\mathrm{U}}c_{\mathrm{U}}l_{\mathrm{L}}\cos(\theta_{\mathrm{U}} - \theta_{\mathrm{L}})$$

$$C'_{\mathrm{MM}} = m_{\mathrm{M}}c_{\mathrm{M}}^2 + m_{\mathrm{U}}l_{\mathrm{M}}^2 + I_{\mathrm{M}}$$

$$C'_{\mathrm{ML}} = C'_{\mathrm{LM}} = (m_{\mathrm{M}}c_{\mathrm{M}}l_{\mathrm{L}} + m_{\mathrm{U}}l_{\mathrm{L}}l_{\mathrm{M}})\cos(\theta_{\mathrm{M}} - \theta_{\mathrm{L}})$$

$$C'_{\mathrm{LL}} = m_{\mathrm{L}}c_{\mathrm{L}}^2 + (m_{\mathrm{M}} + m_{\mathrm{U}})l_{\mathrm{L}}^2 + I_{\mathrm{L}}$$

$$D'_{\mathrm{UU}} = m_{\mathrm{U}}c_{\mathrm{U}}g\sin(\theta_{\mathrm{U}})/\theta_{\mathrm{U}}$$

$$D'_{\mathrm{MM}} = (m_{\mathrm{M}}c_{\mathrm{M}} + m_{\mathrm{U}}l_{\mathrm{M}})g\sin(\theta_{\mathrm{M}})/\theta_{\mathrm{M}}$$

$$D'_{\mathrm{LL}} = (m_{\mathrm{L}}c_{\mathrm{L}} + (m_{\mathrm{M}} + m_{\mathrm{U}})l_{\mathrm{L}})g\sin(\theta_{\mathrm{L}})/\theta_{\mathrm{L}}$$

$$D'_{\mathrm{UM}} = D'_{\mathrm{UL}} = D'_{\mathrm{MU}} = D'_{\mathrm{UM}} = D'_{\mathrm{LU}} = D'_{\mathrm{LM}} = 0$$

$$A'_{\mathrm{U}} = m_{\mathrm{U}}c_{\mathrm{U}}(l_{\mathrm{L}}\sin(\theta_{\mathrm{U}} - \theta_{\mathrm{L}})\dot{\theta}_L^2 + l_{\mathrm{M}}\sin(\theta_{\mathrm{U}} - \theta_{\mathrm{M}})\dot{\theta}_{\mathrm{M}}^2)$$

$$A'_{\mathrm{M}} = (m_{\mathrm{M}}c_{\mathrm{M}}l_{\mathrm{L}} + m_{\mathrm{U}}l_{\mathrm{L}}l_{\mathrm{M}})\sin(\theta_{\mathrm{M}} - \theta_{\mathrm{L}})\dot{\theta}_{\mathrm{L}}^2 - m_{\mathrm{U}}c_{\mathrm{U}}l_{\mathrm{M}}\sin(\theta_{\mathrm{U}} - \theta_{\mathrm{M}})\dot{\theta}_{\mathrm{U}}^2$$

$$A'_{\mathrm{L}} = -(m_{\mathrm{M}}c_{\mathrm{M}}l_{\mathrm{L}} + m_{\mathrm{U}}l_{\mathrm{L}}l_{\mathrm{M}})\sin(\theta_{\mathrm{M}} - \theta_{\mathrm{L}})\dot{\theta}_{\mathrm{M}}^2 - m_{\mathrm{U}}c_{\mathrm{U}}l_{\mathrm{L}}\sin(\theta_{\mathrm{U}} - \theta_{\mathrm{L}})\dot{\theta}_{\mathrm{U}}^2$$

where the parameters $m, I, l$, and $c$ for each of the three body segments are its mass, moment of inertia about the center of mass, length, and distance of segment center of mass from its distal end, respectively. Subscript $i$ applied to the body segment indicates the lower ($i = \mathrm{L}$, shanks), middle ($i = \mathrm{M}$, thighs), and upper ($i = \mathrm{U}$, trunk with arms and head) segments.

Motion equation (1) is written in terms of joint angles $\varphi$ and can be easily obtained from (A1) by the change of variables $\theta = \mathbf{U}\varphi$ where $\mathbf{U} = (\mathbf{N}^{-1})^{\mathrm{T}}$. Then $\mathbf{C}(\varphi) = \mathbf{U}^{\mathrm{T}}\mathbf{C}'(\theta)\mathbf{U}$,

$$\mathbf{D}(\varphi) = \mathbf{U}^{\mathrm{T}}\mathbf{D}'(\theta)\mathbf{U}, \text{ and } \mathbf{A}(\varphi\dot{\varphi}) = \mathbf{U}^{\mathrm{T}}\mathbf{A}'(\theta,\dot{\theta}) \ .$$

In the linear approximation about the erect body position, the motion equation (1) takes the form (2), where $\mathbf{C} = \mathbf{C}(0), \mathbf{D} = \mathbf{D}(0)$ and $\mathbf{A} = 0$.

## Appendix B: The validity of the linear approximation

Since linear approximation allows any movement to be decomposed into the eigenmovements of motion equation, the validity of the linear approximation was estimated for each of the three eigenmovements separately. The movement time course $\xi_i(t)$ along the $i$th eigenvector in the linear approximation was assumed to have a "typical" bell-shaped velocity profile given by (10). Then "linear" joint angles $\varphi_{\mathrm{L}}$ and torques $\mathbf{T}_{\mathrm{L}}$ were calculated by *linear* equations (4), (5), and (6). Thereafter, a direct, dynamic task was solved by the *nonlinear* motion equation (1) under the given joint torques $\mathbf{T}_{\mathrm{L}}$, and under boundary conditions $\dot{\varphi}_{\mathrm{NL}}(0) = \dot{\varphi}_{\mathrm{NL}}(\tau) = 0$. The obtained "nonlinear" joint angles $\varphi_{\mathrm{NL}}$ were then compared with $\varphi_{\mathrm{L}}$ and the accuracy of the linear approximation was estimated by the mean square root error

**Table A1.** Coefficients $E$ (in rad$^{-2}$) for the errors between direct solution of nonlinear motion (1) and its solution when angular dependence of matrices **C** and **D** is ignored ($E_1$), when centripetal and Coriolis forces are ignored ($E_2$), or when both nonlinear effects are ignored ($E_T$) for each eigenmovement

| Eigenmovement list | $\tau$ = 250 ms | | | $\tau$ = 500 ms | | | $\tau$ = 1000 ms | | |
|---|---|---|---|---|---|---|---|---|---|
| | $E_1$ | $E_2$ | $E_T$ | $E_1$ | $E_2$ | $E_T$ | $E_1$ | $E_2$ | $E_T$ |
| A-eig. | 0.11 | 0.53 | 0.55 | 0.10 | 0.14 | 0.21 | 0.11 | 0.04 | 0.13 |
| H-eig. | 0.22 | 0.24 | 0.07 | 0.05 | 0.06 | 0.04 | 0.03 | 0.02 | 0.04 |
| K-eig. | 0.21 | 0.18 | 0.15 | 0.05 | 0.05 | 0.05 | 0.01 | 0.01 | 0.02 |

$$\varepsilon = \sqrt{\frac{1}{\tau}\int_0^{\tau} \sum_{i=\mathrm{A,H,K}} (\varphi_{\mathrm{L}^i} - \varphi_{\mathrm{NL}^i})^2 \mathrm{d}t}$$

In general, linear approximation results in two kinds of errors. The first one ($\varepsilon_1$) is due to ignoring the angular dependences of matrices **C** and **D**, and the second ($\varepsilon_2$) is due to ignoring the centripetal and Coriolis forces defined by vector **A**. The influence of each of these two nonlinear effects on the accuracy of linear approximation was estimated by solving the motion equation (1), in which only one nonlinear effect was taken into account. The total error $\varepsilon_T$ was calculated when both nonlinear effects were taken into account.

As seen from the expressions for the components of matrices **C** and **D**, and of vector **A** given in Appendix A, for small movement amplitudes $\Delta$, the error between linear and nonlinear approximation is proportional to $\Delta^3$.

Table A1 shows coefficients of proportionality $E_1$, $E_2$, and $E_T$ (in rad$^{-2}$) for each eigenmovement A, H, and K and for different movement durations $\tau$. In each eigenmovement, the total error decreases when the movement duration increases. Interestingly, in H-eigenmovement for small movement durations $\tau$, the two nonlinear effects partially compensate each other so that the total error coefficient $E_T$ is less than $E_1$ and $E_2$.

As is shown in Alexandrov et al. (2001) the experimentally observed amplitudes and durations of eigenmovements were on average 4.1° and 820 ms for A-eigenmovement, 65.2° and 510 ms for H-eigenmovement, and 7.4° and 450 ms for K-eigenmovement. Thus according to Table A1, the total errors amount on average to only 0.04%, 3.8%, and 0.1% of the amplitude of A-, H-, and K-eigenmovements, respectively. It is noteworthy that the estimation of the total error $\varepsilon_T \approx E_T\Delta^3$ appeared to be valid even up to $\Delta = 55°$.

## Appendix C: CG and CP displacements

The anteroposterior CG position is given by

$$\begin{aligned} X^{\mathrm{CG}} = -((&m_{\mathrm{L}}c_{\mathrm{L}} + m_{\mathrm{M}}l_{\mathrm{M}} + m_{\mathrm{U}}l_{\mathrm{U}})\sin(\varphi_{\mathrm{A}}) \\ &+ (m_{\mathrm{M}}c_{\mathrm{M}} + m_{\mathrm{U}}l_{\mathrm{U}})\sin(\varphi_{\mathrm{A}} + \varphi_{\mathrm{K}}) \\ &+ m_{\mathrm{U}}c_{\mathrm{U}}\sin(\varphi_{\mathrm{A}} + \varphi_{\mathrm{K}} + \varphi_{\mathrm{H}}))/M \end{aligned}$$

where $M$ is the whole body mass. The subscripts A, K and H indicate ankle, knee and hip joints. Positive $X^{\mathrm{CG}}$ corresponds to the forward CG displacement.

The time course of CP displacement in the anteroposterior direction, $X^{\mathrm{CP}}$, is defined by ankle joint torque $T_{\mathrm{A}}$ and support forces

$$X^{\mathrm{CP}} = (T_{\mathrm{A}} - hF_{\mathrm{X}})/F_{\mathrm{Y}} \tag{C2}$$

where $T_{\mathrm{A}}$ is the torque at the ankle joint, $h$ is the height of the foot (Fig. 1), $F_{\mathrm{X}} = M\ddot{X}^{\mathrm{CG}}$ and $F_{\mathrm{Y}} = M(g + \ddot{Y}^{\mathrm{CG}})$ are the anteroposterior and vertical reaction forces, and $g$ is the gravity acceleration.

In the linear approximation $X^{\mathrm{CG}} = \mathbf{B}^{\mathrm{T}}\varphi$, where $\mathbf{B}^{\mathrm{T}} = -\mathbf{D}_{\mathrm{A}}^{\mathrm{T}}/(Mg)$ and $\mathbf{D}_{\mathrm{A}}^{\mathrm{T}}$ is the first row of the gravitational matrix **D** (see Appendix A). According to (C1)

$$\begin{aligned} B_{\mathrm{A}} = -(&m_{\mathrm{L}}c_{\mathrm{L}} + m_{\mathrm{M}}l_{\mathrm{M}} + m_{\mathrm{U}}l_{\mathrm{U}} + m_{\mathrm{M}}c_{\mathrm{M}} \\ &+ m_{\mathrm{U}}l_{\mathrm{U}} + m_{\mathrm{U}}c_{\mathrm{U}})/M \ , \end{aligned}$$

$$B_{\mathrm{K}} = -(m_{\mathrm{M}}c_{\mathrm{M}} + m_{\mathrm{U}}l_{\mathrm{U}} + m_{\mathrm{U}}c_{\mathrm{U}})/M \ ,$$

$$B_{\mathrm{H}} = -m_{\mathrm{U}}c_{\mathrm{U}}/M \ ,$$

The CG position in each eigenmovement is defined by (8), where according to (4) $b_i = \mathbf{B}^{\mathrm{T}}\mathbf{w}_i (i = \mathrm{A, K, H})$.

Equation (C2) in the linear approximation takes the form

$$X^{\mathrm{CP}} = (T_{\mathrm{A}} - hF_{\mathrm{X}})/(Mg) \tag{C3}$$

In each eigenmovement

$$F_{\mathrm{X}i} = M\ddot{X}_i^{\mathrm{CG}} = Mb_i\ddot{\xi}_i \tag{C4}$$

and according to (5) and (6)

$$\begin{aligned} T_{\mathrm{A}i} = Mgb_i\eta_i &= Mgb_i(-\lambda_i\ddot{\xi}_i + \xi_i) \\ &= Mg(-\lambda_i\ddot{X}_i^{\mathrm{CG}} + X^{\mathrm{CG}}) \end{aligned} \tag{C5}$$

Putting (C4) and (C5) into (C3), one obtains (7).

## References


Alexandrov AV, Frolov AA, Massion J (1998) Axial synergies during upper trunk bending. Exp Brain Res 118: 210–220

Alexandrov AV, Frolov AA, Massion J (2001) Biomechanical analysis of movement strategies in human forward trunk bending. II. Experimental study. Biol Cybern 84: 435–443

Barin K (1989) Evaluation of a generalized model of human postural dynamics and control in the sagittal plane. Biol Cybern 61: 37–50

Babinski J (1899) De l'asynergie cerebelleuse. Rev Neurol (Paris) 7: 806–816

Bizzi E, Hogan N, Mussa-Ivaldi FA, Giszter S (1992) Does the nervous system use equilibrium-point control to guide single and multiple joint movements. Behav Brain Sci 15: 603–613

Bouisset S, Zattara M (1987) Biomechanical study of the programming of anticipatory postural adjustments associated with voluntary movement. J Biomech 20: 735–742

Crenna P, Frigo C, Massion J, Pedotti A (1987) Forward and backward axial synergies in man. Exp Brain Res 65: 538–548

Crenna P, Frigo C, Massion J, Pedotti A, Deat A (1988) Forward and backward axial movements: two modes of central control. In: Gurfinkel VS, Ioffe ME, Massion J, Roll JP (eds) Stance and motion, facts and concepts. Plenum Press, New York, pp 195–201

Do MC, Gilles M (1992) Effects of reducing plantar support on anticipatory postural and intentional activities associated with flexion of the lower limb. Neurosci Lett 148: 181–184

Domen K, Latash ML, Zatsiorsky VM (1999) Reconstruction of equilibrium trajectories during whole-body movements. Biol Cybern 80: 195–204

Eng JJ, Winter DA, MacMinnon CD, Patla AE (1992) Interaction of the reactive moments and center of mass displacement for postural control during voluntary arm movments. Neurosci Res Comm 11: 73–80

Feldman AG, Levin MF (1995) The origin and use of postural frames of reference in motor control. Behav Brain Sci 18: 723–806

Gurfinkel VS (1973) Physical foundations of stabilography. Agressologie 14C: 9–14

Kawato M, Furukawa K, Suzuki R (1987) A hierarchial neural-network model for control and learning of voluntary movement. Biol Cybern 69: 169–185

Kuo AD, Zajac FE (1993) A biomechanical analysis of muscle strength as a limiting factor in standing posture. J Biomech 26 [Suppl 1]: 137–150

Latash ML (1993) Control of human movement. Human Kinetics, Champaign, Ill.

Massion J (1992) Posture and equilibrium: interaction and coordination. Prog Neurophysiol 38: 35–56

Massion J, Popov K, Fabre J-C, Rage P, Gurfinkel V (1997) Is the erect posture in microgravity based on the control of trunk orientation or center of mass position? Exp Brain Res 114: 384–389

Oddsson L, Thorstensson A (1986) Fast voluntary trunk flexion movements in standing: primary movements and associated postural adjustments. Acta Physiol Scand 128: 341–349

Oddsson L, Thorstensson A (1987) Fast voluntary trunk flexion movements in standing: motor patterns. Acta Physiol Scand 129: 93–106

Oddsson L (1990) Control of voluntary trunk movements in man. Mechanisms for postural equilibrium during standing. Acta Physiol Scand Suppl 110: 1595

Pedotti A, Crenna P, Deat A, Frigo C, Massion J (1989) Postural synergies in axial movements: short and long-term adaptation. Exp Brain Res 74: 3–10

Ramos CF, Stark LW (1990) Postural maintenance during fast forward bending: a model simulation experiment determines the reduced ''trajectory''. Exp Brain Res 22: 651–657

Winter DA (1990) Biomechanics and motor control in human movement, 2nd edn. John Wiley, New York

Yang JF, Winter DA, Wells RP (1990) Postural dynamics in the standing human. Biol Cybern 62: 309–320